

A Substrate for Observing Histidine-Tagged Proteins by High-Speed Atomic Force Microscopy

Daisuke YAMAMOTO^{1), 2)}, Kentaro NOI^{2), 3), 4)} and Teru OGURA^{2), 3), 4)}

(Received December 8, 2016)

Abstract

We have developed a novel substrate that specifically adsorbs histidine (His)-tagged proteins for the observations by high-speed atomic force microscopy. A two-dimensional crystal of streptavidin was used as a carrier of Ni-NTA, onto which the N-terminally His-tagged valosin-containing protein (VCP) was specifically adsorbed. All the carboxyl groups that expose to the surface of the streptavidin molecules are estimated to be conjugated with NTA molecules by our procedure. Therefore, the number of density of Ni-NTA on the crystal surface is presumably a saturating value, which ensures the adsorption of the His-tagged protein thereon. The hexameric ring-structure of adsorbed VCP molecule was imaged by high-speed atomic force microscopy at a molecular resolution on this substrate.

1. Introduction

The high-speed atomic force microscopy (high-speed AFM)¹ is a unique tool for directly observing the conformational changes of proteins at work. The dynamic movements of proteins coupled to their functions have been visualized at a molecular resolution, including walking myosin V², conformational changes of β -subunit of rotorless F₁³, binding and release action of GroES at the ends of cylindrical shaped double ring GroEL⁴. These studies clearly demonstrate that the high-speed AFM is a strong tool for revealing the dynamic structures of functioning proteins at nanometer spatial resolutions.

For the AFM observations, adsorption of the proteins of interest onto a solid substrate is a prerequisite. At the early stage of the development of high-speed AFM, it has already been recognized that controlling the interaction between the proteins and the substrate is important for the observations of dynamic processes of proteins by this method^{5,6}. This is because the nonspecific interactions between the proteins and the substrates frequently modulate the dynamics of the proteins. Moreover, to directly visualize the conformational changes of the proteins by high-speed AFM, the proteins must be in the orientation on the substrate so that the protein

domain of interest is facing to the AFM probe. To overcome these problems, streptavidin two-dimensional crystals have been introduced as a substrate, on which the function and the dynamics of the proteins are little perturbed^{4,5}. Streptavidin is comprised of four identical subunits, each of which specifically binds to biotin molecule with a high affinity⁷. Because streptavidin is virtually devoid of nonspecific interaction with other proteins, the biotinylated proteins are attached onto the streptavidin crystal surface essentially through the streptavidin-biotin interaction. This situation enables the proteins to be oriented on the surface in a specific manner, if the biotin molecules are conjugated at a specific site of the protein^{4,6}.

The streptavidin crystal substrate has only been applied to the observations of biotinylated macromolecules. For the applications to a wide range of proteins, a substrate that attaches proteins by another kind of specific interaction would be useful. A candidate for such a substrate would be a streptavidin crystal that is modified with Ni-NTA. Ni-NTA specifically binds histidine (His)-tagged proteins. The Ni-NTA and His-tag system is widely used for the purification of proteins. For a number of proteins, His-tag can be introduced at an arbitrary position in the primary structure of the proteins by gene engineering technique.

1) Department of Applied Physics, Faculty of Science, Fukuoka University, 8-19-1 Nanakuma, Jonan-ku, Fukuoka 814-0180, Japan

2) CREST, JST, Saitama, 332-0012, Japan

3) Department of Molecular Cell Biology, Institute of Molecular Embryology and Genetics, 2-2-1 Honjo, Chuo-ku, Kumamoto University, Kumamoto 860-0811, Japan

4) The Global COE, Kumamoto University, 2-2-1 Honjo, Chuo-ku, Kumamoto 860-0811, Japan

Moreover, Ni-NTA interacts with the His-tag region with a high affinity, while weakly in a nonspecific manner with proteins. Thus, it is expected that the His-tagged proteins will be specifically attached onto the surface of the streptavidin layer that is modified with Ni-NTA in a controlled orientation.

Here, we developed a streptavidin two-dimensional crystal molded with Ni-NTA (NTA-SA crystal), and applied this crystal as a substrate for observing His-tagged proteins by high-speed AFM. In this paper, we used N-terminally His-tagged valosin-containing protein (VCP) as a biological sample. VCP is a member of highly conserved class of AAA+ (ATPases associated with diverse cellular activities) family⁸. VCP is comprised of six identical subunits with a hexameric double-ring structure⁹. The VCP consists of three domains (N-domain, D1 and D2). The N-terminal domain and the D1 domain form N-D1 ring and the D2 domain forms D2 ring, respectively. Our high-speed AFM observations in this study showed that VCP molecules were successively adsorbed onto the NTA-SA crystal surface. Further, our measurements strongly suggest that the adsorption of VCP molecules onto NTA-SA crystal is accomplished essentially by the interaction between His-tag and Ni-NTA. Therefore, the observed ring structure of VCP was attributed to the D2 ring.

2. Materials and methods

2-1. Purification of VCP

The N-terminally His-tagged human VCP was expressed in insect cells and purified as described previously¹⁰. The purified VCP was stored at -80°C until use.

2-2. Conjugation of NTA to streptavidin

Streptavidin was purchased from Wako (Japan). *N*-(5-Amino-1-carboxypentyl)iminodiacetic acid (AB-NTA) was purchased from Dojin (Japan). *N*-Hydroxysulfosuccinimide (sulfo-NHS) and *N*-(3-Dimethylaminopropyl)-*N*'-ethylcarbodiimide hydrochloride (EDC) were from Sigma Aldrich (USA).

NTA was conjugated to streptavidin as follows. Streptavidin was dissolved in a reaction solution containing 100 mM HEPES-KOH (pH7.4), 150 mM KCl, 10 mM AB-NTA, 20 mM sulfo-NHS and 15 mM EDC, and then incubated for more than 2 hours at room temperature to ensure the conjugation reaction between streptavidin and AB-NTA. To remove the unreacted reagents, the sample was dialyzed against a buffer containing 100 mM HEPES-

KOH and 150 mM KCl (pH 7.4). The NTA-modified streptavidin was stored at -80°C until use.

2-3. Evaluation of the number of NTA conjugated to a streptavidin tetramer

The absorption spectrum of Ni in solution shows alteration upon binding to NTA. We utilized this absorption change for the evaluation of the number of NTA molecules conjugated to a streptavidin tetramer. The NTA-modified streptavidin sample was added by an aliquot of NiCl_2 solution, while the absorption changes of the solution were monitored at a wavelength of 1038 nm (see result). The number of NTA molecules conjugated to the streptavidin tetramer was calculated from the titration curve of the absorption change at 1038 nm. The absorption spectra were measured using UV-vis spectrometer UV-1800 (Shimadzu, Japan).

2-4. Preparation of NTA-SA crystal

Streptavidin is known to form two-dimensional crystals on the surface of biotin-containing planar lipid bilayer^{5,11}. On the contrary, for NTA-conjugated streptavidin, all the effort performed by us failed to form two-dimensional crystals on the lipid bilayer. This is ascribed to the modulations of molecular interactions or steric hindrance that occurred upon the conjugation of extrinsic NTA molecules to streptavidin. Therefore, we first obtained two-dimensional crystal of unconjugated streptavidin, and then NTA was subsequently conjugated to streptavidin in the crystal as follows. Streptavidin two-dimensional crystal on planar lipid bilayer was obtained and chemically fixed with glutaraldehyde as described previously⁵. Subsequently, the streptavidin in the crystal was conjugated with NTA in the reaction solution supplemented with 12.5 mM NiCl_2 .

2-5. High-speed atomic force microscopy

Imaging was performed with a laboratory-built high-speed AFM^{1,12}. The high-speed AFM was equipped with small cantilevers designed for high-speed scanning (spring constants ~ 0.1 N/m, resonant frequencies ~ 600 kHz) and operated in tapping mode. VCP (0.6-0.8 μM hexamer) was loaded onto the NTA-SA crystal and allowed to be attached onto the surface for 15 min to 1 hour. After the unattached VCP was washed out, the sample was imaged by high-speed AFM in 50 mM Tris-HCl, 50 mM KCl and 5 mM MgCl_2 (pH8.0).

3. Results

3-1. Absorption change of Ni upon binding to NTA

At first, we estimated the absorption spectrum change of Ni upon the formation of the complex with NTA. An aliquot of NiCl_2 was added to AB-NTA solution and the absorption spectrum change was monitored (Fig. 1a). The absorbance increased upon the addition of Ni extremely at wavelength of 218 nm, and moderately at 382 nm, 616 nm and 1038 nm, respectively. In addition, a shoulder at the right side of the peak at 616 nm was also observed (753 nm). Fig. 1b shows titration curves of absorption changes observed at each wavelength. The absorbance at each wavelength increased linearly up to a molar ratio of Ni to NTA reached to 1 to 1. At a higher molar ratio, the sensitivity of the absorption change against the Ni addition significantly reduced at 218 nm and 1038 nm, and to some extent at 382 nm and 616 nm. The absorbance increased almost linearly at 753 nm throughout the molar ratio of Ni to NTA tested. Thus, the

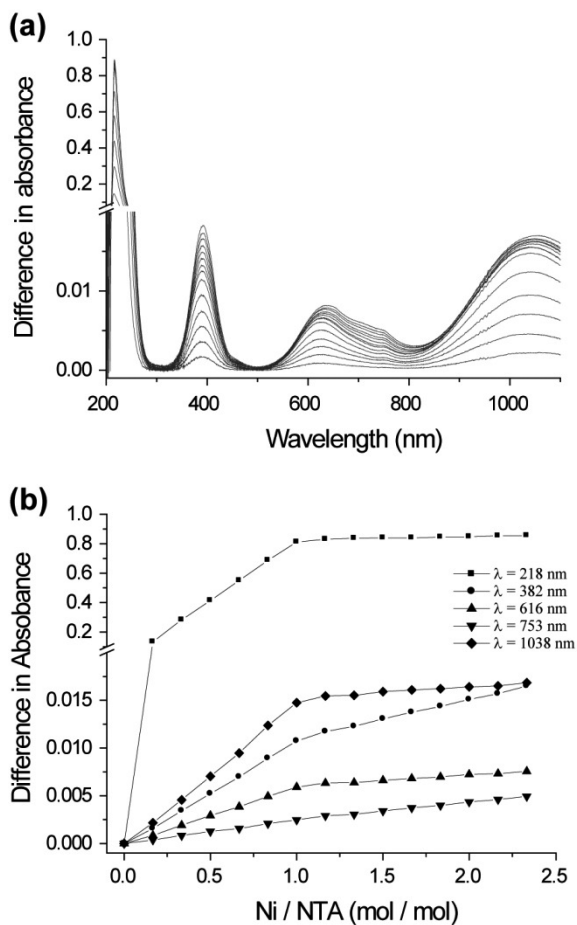


Fig. 1 Absorption change of Ni upon the formation of a complex with NTA. (a) Differential spectrum of NTA solution upon addition of Ni. (b) Titration curves of absorption changes upon addition of Ni at wavelength of 218 nm, 382 nm, 616 nm, 753 nm and 1038 nm.

absorption changes at 218 nm and 1038 nm are essentially induced by the binding of Ni to NTA, and can be used as an indication of the formation of Ni-NTA complex. Obviously, the absorption change at 218 nm showed extremely high sensitivity upon the binding of Ni to NTA. However, streptavidin also shows high absorption efficiency at this wavelength. Therefore, it should be improper to use the wavelength of 218 nm to estimate the formation of Ni-NTA complex. Instead, we used absorption change at 1038 nm for this purpose.

3-2. Evaluation of the number of NTA molecules conjugated to a streptavidin tetramer

Each streptavidin subunit involves nine carboxyl groups (four aspartate, four glutamates and a C-terminal amino acid). Among these, seven carboxyl groups are exposed to the surface (PDB: 1NDJ), at which the AB-NTA molecules potentially can be conjugated through the amide bond with the aid of sulfo-NHS and EDC. Therefore, streptavidin tetramer is expected to reside 28 NTA molecules after the reaction with a saturating condition.

Fig. 2 shows a titration curve of the absorption change at 1038 nm upon the addition of Ni to NTA conjugated streptavidin sample. The plot showed a clear inflection point at a molar ratio of Ni to streptavidin tetramer of 32 (i.e. 32 NTA molecules are conjugated to a streptavidin tetramer). This result indicates that all carboxyl groups exposed to the surface of the streptavidin, and an additional amino acid residue, are conjugated by AB-NTA by our experimental procedure. The additional site that reacted with NTA could be attributed to the glutamate residue that is partially exposed to the surface of streptavidin.

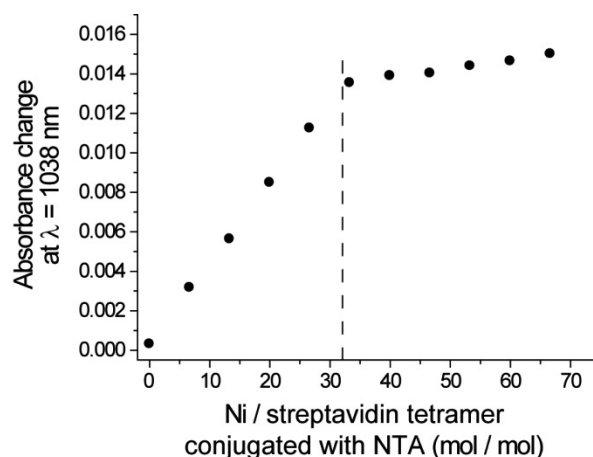


Fig. 2 A titration curve of the absorption change at 1038 nm upon the addition of Ni to streptavidin conjugated with NTA. The dotted line indicates the position at the molar ratio of Ni to streptavidin tetramer of 32.

3-3. High-speed AFM observations of N-terminally His-tagged VCP on NTA-SA crystal

Fig. 3 shows a high-speed AFM image of NTA-SA crystal. The structure of streptavidin tetramer within the crystal was clearly observed. The structure of the streptavidin molecules and the lattice constants of the NTA-SA crystal were very similar to that of streptavidin crystal before the conjugation with NTA⁵.

To demonstrate the specificity of the NTA-SA crystal to the binding of the His-tagged proteins, we first applied a non-His-tagged protein, bovine serum albumin, to the surface as a control. Any additional protein structures were never observed in this case, showing the high resistance of the NTA-SA crystal to the non-specific protein adsorption (data not shown).

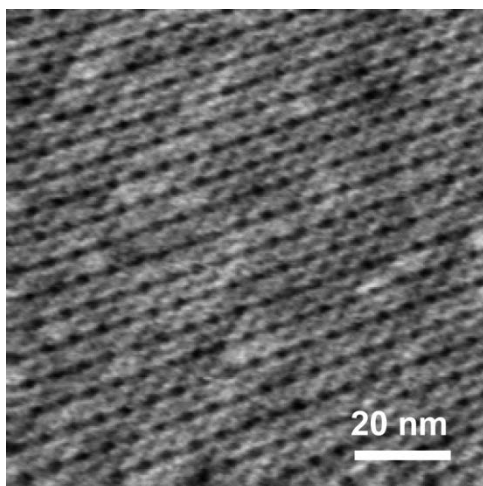


Fig. 3 A high-speed AFM image of NTA-SA crystal. Frame rate: 1 frame/sec. Z-scale: 1.2 nm.

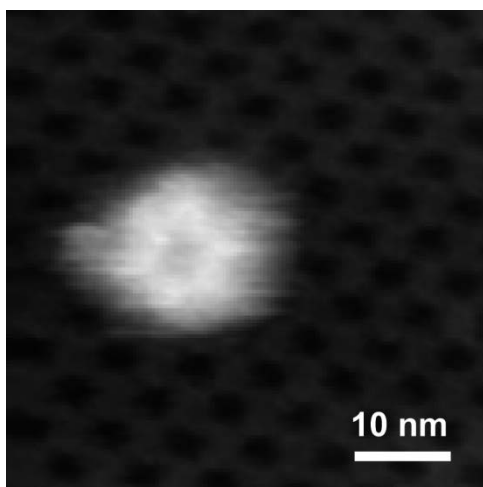


Fig. 4 A high-speed AFM image of N-terminally His-tagged VCP adsorbed on the NTA-SA crystal. Frame rate: 1 frame/sec. Z-scale: 12 nm.

Next, the N-terminally His-tagged VCP was applied to the NTA-SA crystal, and subsequently imaged by high-speed AFM at a relatively low frame rate (Fig. 4). A hexameric ring structure was clearly observed on the NTA-SA crystal lattice. The diameter and the height of this structure were consistent with those of the structure of VCP obtained by cryo-electron microscopy⁹. By contrast, the N-terminally His-tagged VCP completely failed to be attached to the streptavidin crystal that is devoid of the NTA conjugation as observed by high-speed AFM (data not shown). Therefore, it is most plausible that the N-D1 ring of VCP is interacting with NTA-SA crystal through the binding between His-tag and Ni-NTA. Thus, the observed ring-like structure was attributed to the D2 ring of VCP, while the N-D1 ring of VCP is facing to the crystal.

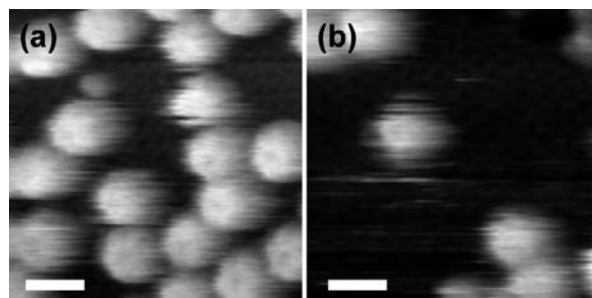


Fig. 5 Desorption of His-tagged VCP from NTA-SA crystal induced by an addition of imidazole. High-speed AFM images of VCP before (a) and after (b) the incubation in the presence of imidazole. Frame rate: 1 frame/sec. Scale bars: 20 nm. Z-scales: 12 nm.

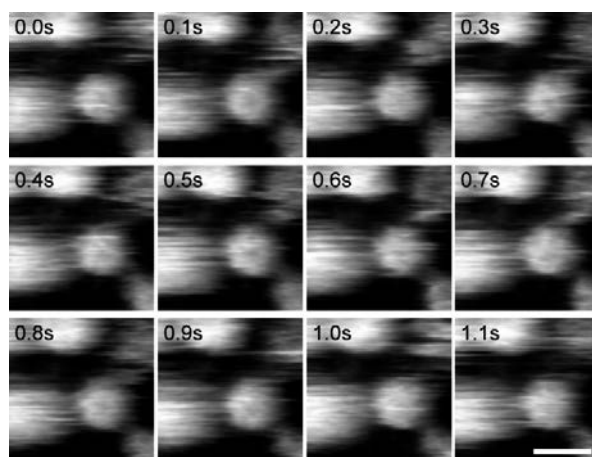


Fig. 6 Successive high-speed AFM images of N-terminally His-tagged VCP on NTA-SA crystal in the presence of 0.3 mM ATP. Frame rates: 10 frames/sec. Scale bar: 20 nm. Z-scale: 12 nm.

To further confirm that the VCP is interacting with the NTA-SA crystal through His-tag, the VCP molecules adsorbed on the crystal was incubated in a buffer containing 300 mM imidazole. After the incubation with imidazole, the number density of VCP molecule was largely decreased (Fig. 5), showing that a significant fraction of VCPs were desorbed from the NTA-SA crystal surface by substituting the binding of Ni-NTA from with His-tag to with imidazole molecules.

To directly observe the conformational changes of the D2 ring during its ATPase cycle, we carried out high-speed AFM imaging (10 frames/sec) of VCP on NTA-SA crystal in the presence of ATP. However, the VCP molecules fluctuated under the scanning tip at this frame rate (Fig. 6), which hampered the high-speed AFM imaging at a high resolution that is sufficient to detect the conformational changes of the D2 ring.

4. Discussion

In this paper, we described a novel substrate that specifically adsorbs His-tagged proteins. The flatness of NTA-SA crystal developed in this study was comparable to that of the two-dimensional crystal of streptavidin that is devoid of NTA conjugation⁵ (Fig. 3). This property of the substrate is an important factor to unambiguously identify the proteins of interest on the surface. Almost all carboxyl groups in the streptavidin were estimated to be conjugated with NTA with our procedure (Fig. 2). Therefore, the number density of Ni-NTA at the surface of NTA-SA is presumably a saturating value, ensuring the adsorption of His-tagged VCP onto the substrate through the interaction between the His-tag and the Ni-NTA (Fig. 4 and 5). Furthermore, the His-tagged proteins appear to be adsorbed onto the substrate with a unique orientation, because their interaction essentially occurs at the interface of Ni-NTA and His-tagged region of the protein. We used N-terminally His-tagged VCP in this study, therefore the observed ring-like hexameric structure was attributed to the D2 ring. The observations of the opposite side of VCP, the N-D1 ring, on NTA-SA crystal will be accomplished by the use of C-terminally His-tagged VCP.

A previous high-speed AFM imaging revealed the back and forth rotational movement of N-D1 ring of CDC-48 from *Caenorhabditis elegans*, a homologue of human VCP, on bare mica¹³. This conformational change of N-D1 ring couples to the binding of ATP at the D2 ring of CDC-48. However, the ATPase rate of CDC-48 on mica surface is

significantly reduced compared to that in the bulk solution. This may be ascribed to the multiple site interaction between the D2 ring of CDC-48 and the mica surface, which will modulate the binding affinity of ATP to the D2. One potential means to circumvent this issue would be the use of NTA-SA crystal.

We could not achieve the high-speed AFM imaging of VCP with a high spatial and temporal resolution that is sufficient to analyze the dynamic conformational change of the D2 ring during its ATPase cycle (Fig. 6). This was largely because of the fluctuation of VCP molecules under the scanning tip at a frame rate of 10 frames/sec. The each subunit of the N-terminally His-tagged VCP contains a flexible region between the His-tag and the N-D1 ring. Therefore, the VCP molecules intrinsically thermally fluctuate on the NTA-SA crystal surface, which will be enhanced by the interaction with the rapidly scanning probe tip of AFM at a high imaging rate. A coupling of charged small molecules to NTA-SA crystal would be one possible strategy to achieve the observations of the conformational changes of the D2 during its ATPase cycle. This additional coulomb interaction will suppress the fluctuation of the VCP on the surface, which will be a suitable situation for high-speed AFM imaging of proteins with a high spatial and temporal resolution.

5. Conclusions

We have developed a novel substrate that specifically adsorbs His-tagged proteins for high-speed AFM measurements. The N-terminally His-tagged VCP molecules were successfully attached to the surface through the binding between His-tag and Ni-NTA, which enabled us to directly visualize the D2 ring of VCP. However, a high-speed AFM observation of conformational changes of the D2 during its ATPase cycle was not achieved, due to the fluctuation of VCP molecules on the surface. Therefore, further effort is needed to optimize the interaction between the proteins and the substrate.

Acknowledgements

This work was supported by the CREST program of the Japan Science and Technology Agency (JST) and the program of the Joint Usage/Research Center for Developmental Medicine, Institute of Molecular Embryology and Genetics, Kumamoto University.

References

- 1 Ando, T. et al. A high-speed atomic force microscope for studying biological macromolecules. *Proc. Natl. Acad. Sci. U.S.A.* **98**, 12468-12472 (2001).
- 2 Kodera, N., Yamamoto, D., Ishikawa, R. & Ando, T. Video imaging of walking myosin V by high-speed atomic force microscopy. *Nature* **468** (2010).
- 3 Uchihashi, T., Iino, R., Ando, T. & Noji, H. High-speed atomic force microscopy reveals rotary catalysis of rotorless F₁-ATPase. *Science* **333**, 755-758 (2011).
- 4 Yamamoto, D. & Ando, T. Chaperonin GroEL-GroES functions as both alternating and non-alternating engines. *J. Mol. Biol.* **428**, 3090-3101 (2016).
- 5 Yamamoto, D., Nagura, N., Omote, S., Taniguchi, M. & Ando, T. Streptavidin 2D crystal substrates for visualizing biomolecular processes by atomic force microscopy. *Biophys. J.* **97**, 2358-2367 (2009).
- 6 Yamamoto, D. et al. High-Speed atomic force microscopy techniques for observing dynamic biomolecular processes. *Methods Enzymol.* **475**, 541-564 (2010).
- 7 Green, N. M. Avidin and streptavidin. *Methods Enzymol.* **184**, 51-67 (1990).
- 8 Ogura, T. & Wilkinson, A. J. AAA+ superfamily ATPase: common structure-diverse function. *Genes to Cells* **6**, 575-597 (2001).
- 9 Banerjee, S. et al. 2.3 Å resolution cryo-EM structure of human p97 and mechanism of allosteric inhibition. *Science* **351**, 871-875 (2016).
- 10 Nishikori, S., Esaki, M., Yamanaka, K., Sugimoto, S. & Ogura, T. Positive cooperativity of the p97 AAA ATPase is critical for essential functions. *J. Biol. Chem.* **286**, 15815-15820 (2011).
- 11 Reviakine, I. & Brisson, A. Streptavidin 2D crystals on supported phospholipid bilayers: Toward constructing anchored phospholipid bilayers. *Langmuir* **17**, 8293-8299 (2001).
- 12 Ando, T., Uchihashi, T. & Fukuma, T. High-speed atomic force microscopy for nano-visualization of dynamic biomolecular processes. *Prog. Surf. Sci.* **83**, 337-437 (2008).
- 13 Noi, K. et al. High-speed atomic force microscopic observation of ATP-dependent rotation of the AAA+ chaperone p97. *Structure* **21**, 1992-2002 (2013).